

Electronic Supplementary Information

Hydrothermal topotactic epitaxy of SrTiO₃ on Bi₄Ti₃O₁₂ nanoplatelets: understanding the interplay of lattice mismatch and supersaturation

Alja Čontala, Nina Daneu, Suraj Gupta, Matjaž Spreitzer, Anton Meden and Marjeta Maček Kržmanc*

Table S1: Final concentrations (c) of reagents before hydrothermal reaction at 200 °C

C _{Bi₄Ti₃O₁₂} (mol/l)	Initial Sr/Ti ratio	C _{SrCl₂x6H₂O} (mol/L)	C _{NaOH} (mol/L)
0.00102	1:1	0.00306	2 and 6
	3:1	0.00918	
	12:1	0.03672	
	24:1	0.07344	

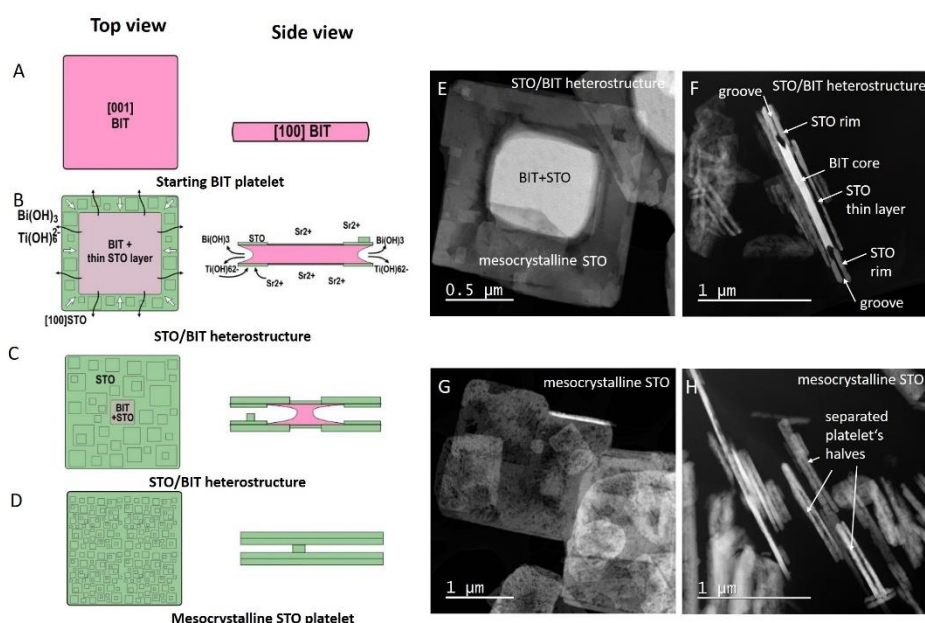


Figure S1: (A-D) schematic presentation of the Bi₄Ti₃O₁₂-to-SrTiO₃ transformation from the top and side view: (A) ⇒ initial Bi₄Ti₃O₁₂ (BIT) platelets, (B, C) ⇒ SrTiO₃/Bi₄Ti₃O₁₂ (STO/BIT) heterostructural platelets at different stages of the transformation, (D) SrTiO₃ (STO) platelets. (E-H) STEM micrographs of the (E, F) heterostructural SrTiO₃/Bi₄Ti₃O₁₂ (STO/BIT) platelets and (G, H) SrTiO₃ platelets from the top (E, G) and side view (F, H). The STEM micrographs, shown in E and F, and those presented in G and H, correspond to the to the transformation schematically presented at B and D, respectively.¹

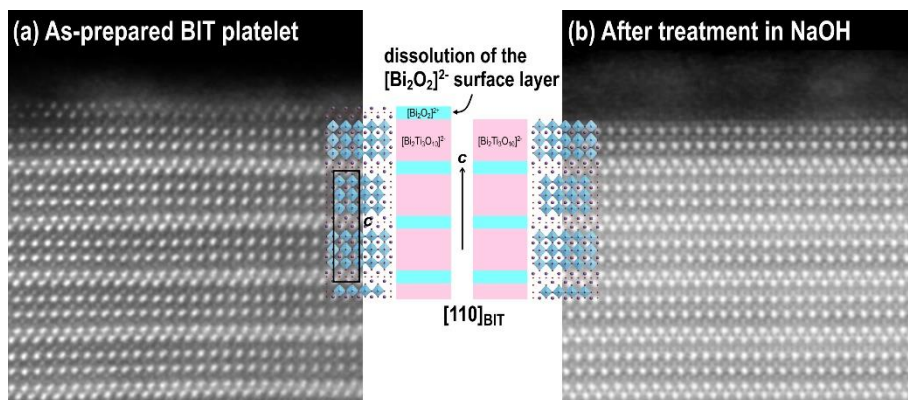


Figure S2: Cross-sectional HAADF-HR-STEM images of the $\text{Bi}_4\text{Ti}_3\text{O}_{12}$ (BIT) platelet in the $[110]$ orientation taken near the surface of the platelets with overlaid structural models: (a) As-prepared $\text{Bi}_4\text{Ti}_3\text{O}_{12}$ (BIT) platelets, terminated by bismuth oxide $[\text{Bi}_2\text{O}_2]^{2-}$ layer (the black rectangular denotes the unit cell of $\text{Bi}_4\text{Ti}_3\text{O}_{12}$) and (b) $\text{Bi}_4\text{Ti}_3\text{O}_{12}$ (BIT) platelets after exposure to hot NaOH (6 mol/L NaOH, holding time 1 hour at 200°C), terminated by pseudoperovskite ($[\text{Bi}_2\text{Ti}_3\text{O}_{10}]^{2-}$) blocks.

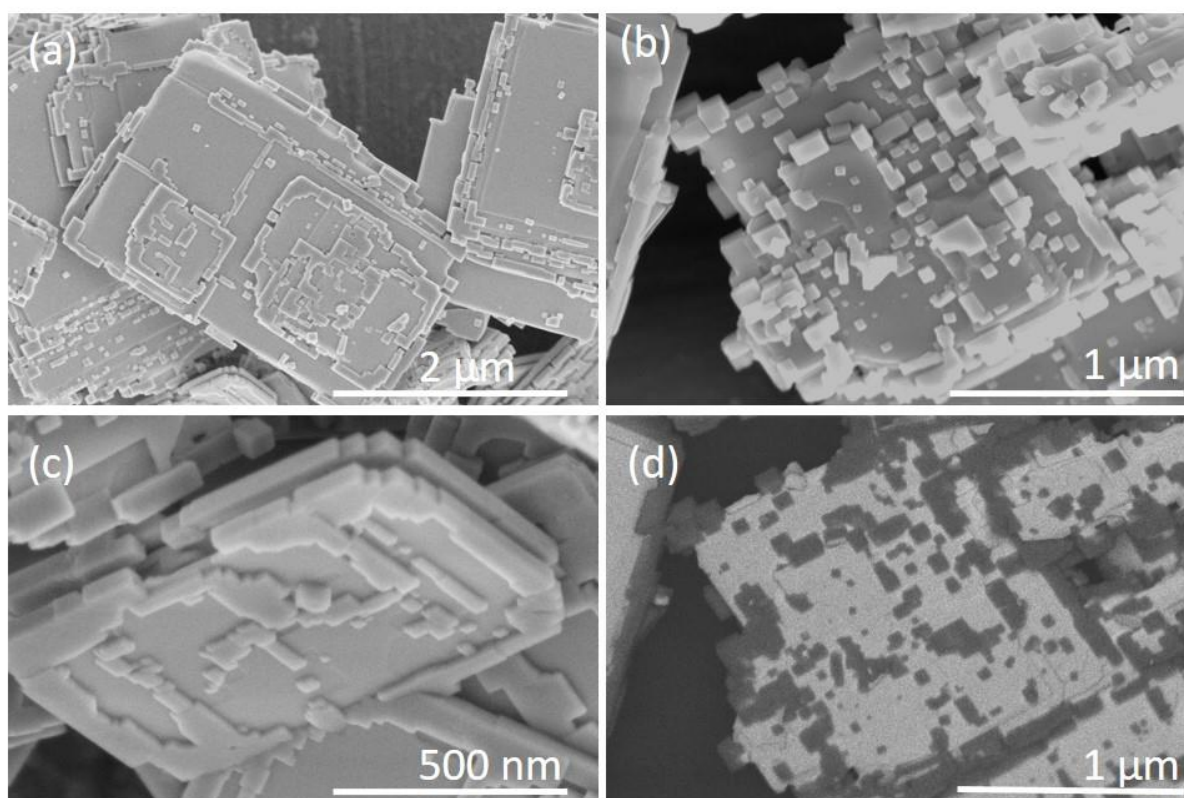


Figure S3: SEM micrographs (a-c secondary electron (SE) images) of the $\text{SrTiO}_3/\text{Bi}_4\text{Ti}_3\text{O}_{12}$ platelets after 2.5 h at 200°C at $\text{Sr}/\text{Ti}=1$ in 2 mol/l NaOH. Image (d) is backscattered (BSE) image of the image shown in (b).

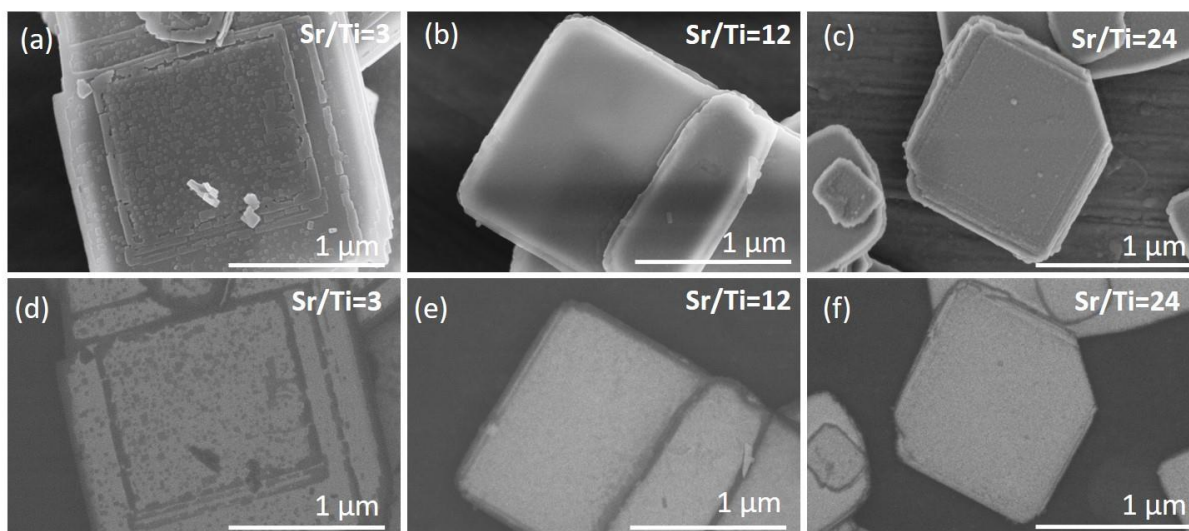


Figure S4: SEM micrographs (SE images: **a,b,c** and BSE images: **d,e,f**) of the $\text{SrTiO}_3/\text{Bi}_4\text{Ti}_3\text{O}_{12}$ platelets after 2.5 h at 200 °C in 2 mol/l NaOH at various Sr/Ti ratios: (**a, d**) Sr/Ti=3, (**b, e**) Sr/Ti=12, (**c, f**) Sr/Ti=24.

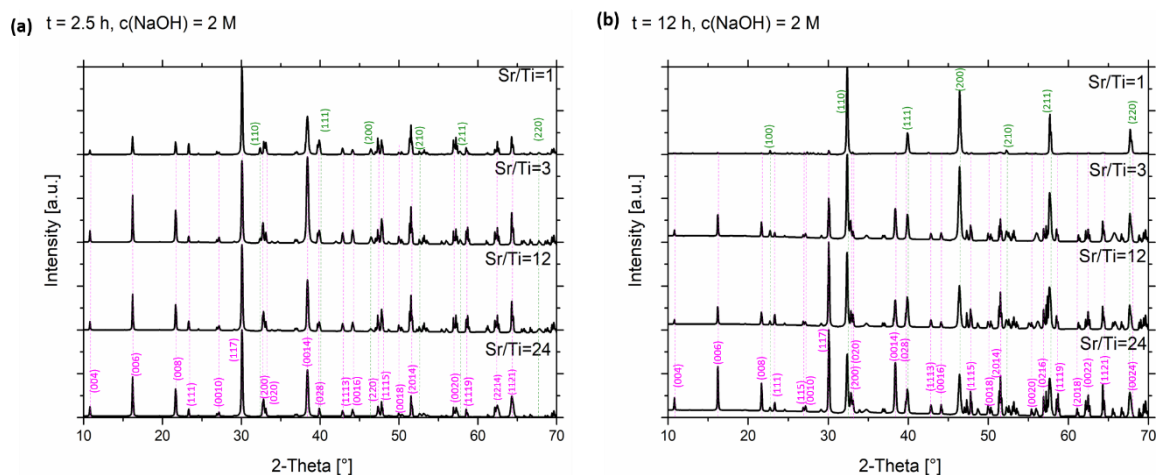


Figure S5: Powder XRD patterns (2θ : 10 °-70 °) of $\text{SrTiO}_3/\text{Bi}_4\text{Ti}_3\text{O}_{12}$ and SrTiO_3 reaction product after 2.5 h and 1 2h at 200 °C in 2 mol/L NaOH at different Sr/Ti ratios. The XRD patterns were indexed with JCPDS reference cards 01-074-1296 and 01-072-1019 for SrTiO_3 (STO) and $\text{Bi}_4\text{Ti}_3\text{O}_{12}$ (BIT), respectively.

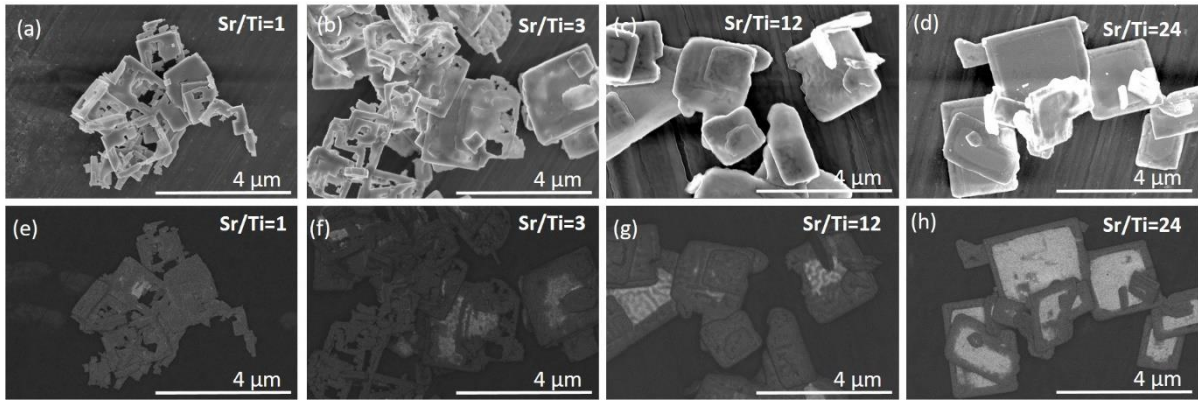


Figure S6: SEM micrographs of the SrTiO₃ structures and SrTiO₃/Bi₄Ti₃O₁₂ platelet after 12 h reaction at 200 °C in 2 mol/L NaOH and at different Sr/Ti ratios (a-d: SE images, e-h: corresponding BSE images).

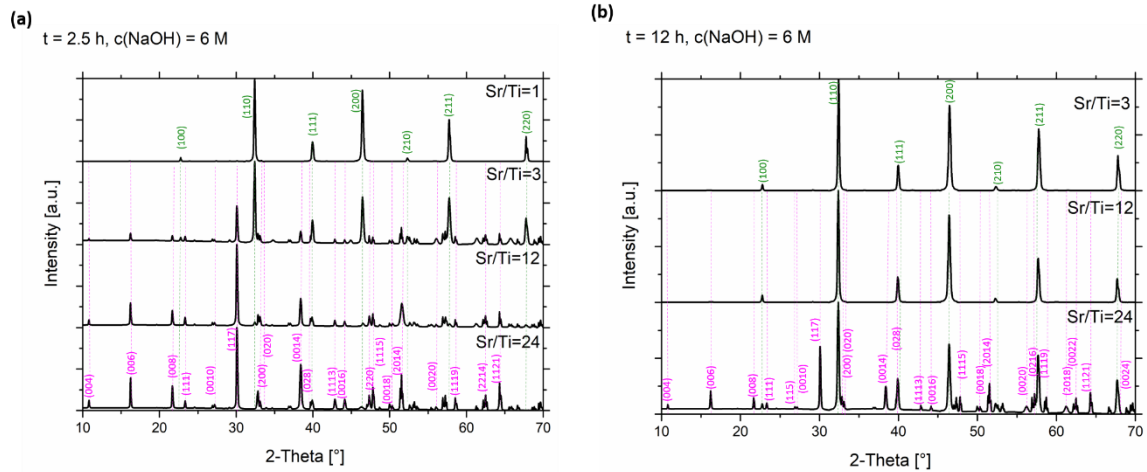


Figure S7: Powder XRD patterns (2θ : 10 °-70 °) of SrTiO₃/Bi₄Ti₃O₁₂ and SrTiO₃ reaction product after 2.5 h and 12 h at 200 °C in 6 mol/L NaOH at different Sr/Ti ratios. The XRD patterns were indexed with JCPDS reference cards 01-074-1296 and 01-072-1019 for SrTiO₃ (STO) and Bi₄Ti₃O₁₂ (BIT), respectively.

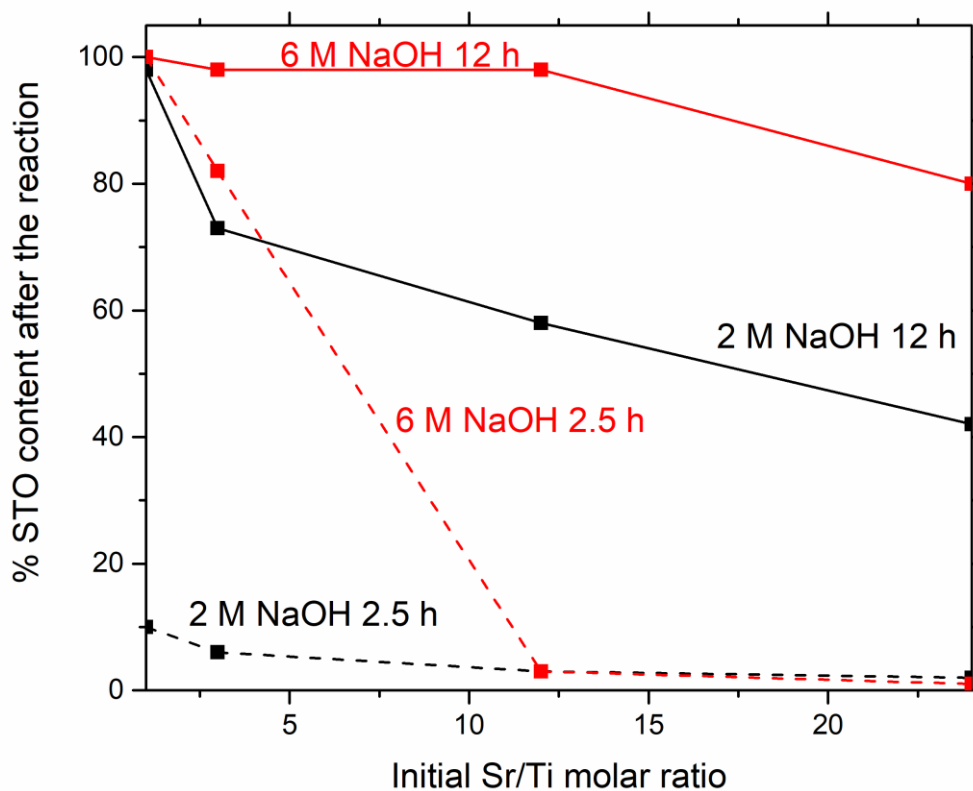


Figure S8: Graphical presentation of the SrTiO₃ (STO) content in percentage after the reaction. The lines are added for visualisation; however, the reactions were performed only for Sr/Ti=1, 3, 12 and 24 molar ratios (the points denoted with squares). The black lines are for the reactions in 2 mol/L NaOH and the red lines are for the reactions in 6 mol/L NaOH. In both cases, dashed lines are for the reactions after 2.5 h and solid for the reactions after 12 h. All reactions were performed at 200 °C.

References

- (1) Maček Kržmanc, M.; Daneu, N.; Čontala, A.; Santra, S.; Kamal, K. M.; Likozar, B.; Spreitzer, M. SrTiO₃/Bi₄Ti₃O₁₂ Nanoheterostructural Platelets Synthesized by Topotactic Epitaxy as Effective Noble-Metal-Free Photocatalysts for PH-Neutral Hydrogen Evolution. *ACS Appl. Mater. Interfaces* **2021**, *13* (1), 370–381. <https://doi.org/10.1021/acsami.0c16253>.